

Compact model for quarks and leptons via flavored axions

Y. H. Ahn*

Key Laboratory of Particle Astrophysics, Institute of High Energy Physics, Chinese Academy of Sciences, Beijing 100049, China

 (Received 30 March 2018; revised manuscript received 10 July 2018; published 31 August 2018)

We show how the scales responsible for the Peccei-Quinn (PQ), seesaw, and Froggatt-Nielsen (FN) mechanisms can be fixed by constructing a compact model to resolve rather recent, but increasingly important issues in astroparticle physics, including quark and leptonic mixings and CP violations, high-energy neutrinos, the QCD axion, and axion cooling of stars. The model is motivated by the flavored-PQ symmetry to unify flavor physics and string theory. The QCD axion decay constant congruent to the seesaw scale—through its connection to the astroparticle constraints of both the stellar evolution induced by the flavored-axion bremsstrahlung off electrons $e + Ze \rightarrow Ze + e + A_i$ and the rare flavor-changing decay process induced by the flavored-axion $K^+ \rightarrow \pi^+ + A_i$ —is shown to be fixed at $F_A = 3.56_{-0.84}^{+0.84} \times 10^{10}$ GeV. Consequently, the QCD axion mass $m_a = 1.54_{-0.29}^{+0.48} \times 10^{-4}$ eV, the Compton wavelength of its oscillation $\lambda_a = 8.04_{-1.90}^{+1.90}$ mm, and the axion-to-neutron coupling $g_{Ann} = 2.14_{-0.41}^{+0.66} \times 10^{-12}$. Subsequently, the scale associated with the FN mechanism is dynamically fixed, $\Lambda = 2.04_{-0.48}^{+0.48} \times 10^{11}$ GeV, through its connection to the standard model fermion masses and mixings, and such a fundamental scale might give a hint of where some string moduli are stabilized in type IIB string vacua. In the near future, the NA62 experiment—which is expected to reach a sensitivity of $\text{Br}(K^+ \rightarrow \pi^+ + A_i) < 1.0 \times 10^{-12}$ —will probe the flavored axions or exclude the model if the astrophysical constraint of star cooling is really responsible for the flavored axion.

DOI: 10.1103/PhysRevD.98.035047

I. INTRODUCTION

Symmetries have always played an important role in physics in general and in quantum field theory in particular. The standard model (SM) as a low-energy effective theory has been very predictive and well tested, due to the symmetries satisfied by the theory, namely, Lorentz invariance plus the $SU(3)_C \times SU(2)_L \times U(1)_Y$ gauge symmetry, in addition to the discrete spacetime symmetries like P and CP . However, it leaves many open questions for theoretical and cosmological issues that have not been solved yet (e.g., Refs. [1,2]). The SM therefore cannot be the final answer. It is widely believed that the SM should be extended to a more fundamental underlying theory. Neutrino mass and mixing is the first new physics beyond the SM and adds an impetus to solve several open questions in astroparticle physics and cosmology. The seesaw mechanism [3] has been the most promising theory to explain neutrino mass. Moreover, a solution

to the strong CP problem of QCD through the Peccei-Quinn (PQ) mechanism [4]¹ may hint at a new extension of gauge theory [1,7]. If the QCD axion as a solution to the strong CP problem exists, it can easily fit into a string-theoretic framework and appear cosmologically as a form of cold dark matter.² The flavor puzzle of the SM charged-fermion mass hierarchies could be solved by implementing the Froggatt-Nielsen (FN) mechanism [9]. If these mechanisms are realized in nature at low energies, finding the scales responsible for the seesaw, PQ, and FN mechanisms could be an important step of resolving these fundamental issues of particle physics and cosmology.

Many of the outstanding mysteries of astrophysics may be hidden at all wavelengths of the electromagnetic spectrum because of absorption by matter and radiation between us and the source, so data from a variety of observational windows—especially through direct observations with neutrinos and axions—may be crucial. Hence, axions and neutrinos in astroparticle physics and

*axionahn@naver.com

Published by the American Physical Society under the terms of the [Creative Commons Attribution 4.0 International license](https://creativecommons.org/licenses/by/4.0/). Further distribution of this work must maintain attribution to the author(s) and the published article's title, journal citation, and DOI. Funded by SCOAP³.

¹See Ref. [5] for some recent related simple toy models [(non) supersymmetric versions]; see also Ref. [6].

²Regarding this issue, we will consider a flavored axion [8] as cold dark matter in a future study. The scale in Eq. (44) that we found is able to explain dark matter, and finding it in experiments could change our fundamental understanding of the Universe.

cosmology could be powerful sources for a new extension of SM particle physics [1,2,7], given their convincing physics and the variety of experimental probes. Fortunately, most recent analyses of neutrinos (low-energy neutrino oscillations [10] and high-energy neutrinos [11]) and axions [the QCD axion [12,13] and an axion-like-particle (ALP) [14,15]] have entered a new phase of model construction for quarks and leptons [8]. In light of finding the fundamental scales, interestingly enough, there are two astroparticle constraints coming from the star cooling induced by the flavored-axion bremsstrahlung off electrons $e + Ze \rightarrow Ze + e + A_i$ [14], and the rare flavor-changing decay process induced by the flavored-axion $K^+ \rightarrow \pi^+ + A_i$ [16], respectively,

$$6.7 \times 10^{-29} \lesssim \alpha_{\text{Aee}} \lesssim 5.6 \times 10^{-27} \quad \text{at } 3\sigma,$$

$$\text{Br}(K^+ \rightarrow \pi^+ A_i) < 7.3 \times 10^{-11}, \quad (1)$$

where α_{Aee} is the fine-structure ratio of the axion to the electron. Since astroparticle physics observations have placed increasingly tight constraints on the parameters for flavored axions, it is important to develop a compact model for quarks and leptons that is able to fix the fundamental scales, such as the scales of the seesaw, PQ, and FN mechanisms. The purpose of the present paper is to construct a flavored-PQ model [8] along these lines, which naturally extends to the compact symmetry $G_F = \text{anomalous } U(1) \text{ plus non-Abelian (finite) symmetries}$ for new physics beyond the SM. We note that [17] in modeling the $U(1)$ mixed-gravitational anomaly cancellation [18] is of central importance in constraining the fermion contents of a new chiral gauge theory and the flavor structure of G_F is strongly correlated with physical observables. Here the flavored-PQ $U(1)$ symmetry together with the non-Abelian finite symmetry is well flavor-structured in a unique way such that the domain-wall number $N_{\text{DW}} = 1$ with the $U(1)_X \times [\text{gravity}]^2$ anomaly-free condition demands additional Majorana fermions and the flavor puzzles of the SM are well delineated by the new expansion parameters expressed in terms of $U(1)_X$ charges and $U(1)_X \times [SU(3)_C]^2$ anomaly coefficients, providing interesting physical implications for neutrinos, the QCD axion, and flavored axions.³

The rest of this paper is organized as follows. In Sec. II we construct a compact model based on $SL_2(F_3) \times U(1)_X$ in a supersymmetric framework. Subsequently, we show that the model works well with the SM fermion mass spectra and their peculiar flavor-mixing patterns. In Sec. III we show that the QCD decay constant (congruent to the seesaw scale) is well fixed through constraints coming from astroparticle physics, and in turn the FN scale is dynamically determined via its connection to the SM fermion

masses and mixings, and we show several properties of the flavored axions. A summary and our conclusions are presented in Sec. IV.

II. FLAVORED $SL_2(F_3) \times U(1)_X$ SYMMETRY

Similar to Ref. [17], we assume that we have a SM gauge theory based on the $G_{\text{SM}} = SU(3)_C \times SU(2)_L \times U(1)_Y$ gauge group, and that the theory has in addition a $G_F \equiv SL_2(F_3) \times U(1)_X$ for a compact description of new physics beyond the SM. Here the symmetry group of the double tetrahedron $SL_2(F_3)$ [20–22] could be realized in field theories on orbifolds; it is a subgroup of a gauge symmetry that can be protected from quantum-gravitational effects. And the $U(1)_X$ as the flavored-PQ symmetry is composed of two anomalous symmetries $U(1)_{X_1} \times U(1)_{X_2}$ generated by the charges $X_1 \equiv -2p$ and $X_2 \equiv -q$. Here the global $U(1)$ symmetry⁴ including $U(1)_R$ is a remnant of the broken $U(1)$ gauge symmetries which can connect string theory with flavor physics [1,7]. Hence, the spontaneous breaking of $U(1)_X$ gives rise to the Nambu-Goldstone (NG) mode (called the axion) and provides an elegant solution to the strong CP problem.

A. Vacuum configuration

We briefly review the field contents responsible for the vacuum configuration since the scalar potential of the model is the same as in Ref. [17]. Apart from the usual two-Higgs doublets $H_{u,d}$ responsible for electroweak symmetry breaking, which transform as $(\mathbf{1}, 0)$ under $SL_2(F_3) \times U(1)_X$ symmetry, the scalar sector is extended via two types of new scalar multiplets that are G_{SM} singlets: flavon fields $\Phi_T, \Phi_S, \Theta, \tilde{\Theta}, \eta, \Psi, \tilde{\Psi}$ responsible for the spontaneous breaking of the flavor symmetry, and driving fields $\Phi_0^T, \Phi_0^S, \eta_0, \Theta_0, \Psi_0$ that break the flavor group along required vacuum expectation value (VEV) directions and allow the flavons to acquire VEVs, which couple only to the flavons. The electroweak Higgs fields $H_{u,d}$ are enforced to be neutral under $U(1)_X$ to avoid the axionic domain-wall problem.

Under $SL_2(F_3) \times U(1)_X$ the flavon fields $\{\Phi_T, \Phi_S\}$ transform as $(\mathbf{3}, 0)$ and $(\mathbf{3}, X_1)$, η transforms as $(\mathbf{2}', 0)$, and $\{\Theta, \tilde{\Theta}, \Psi, \tilde{\Psi}\}$ transform as $(\mathbf{1}, X_1)$, $(\mathbf{1}, X_1)$, $(\mathbf{1}, X_2)$, and $(\mathbf{1}, -X_2)$, respectively; the driving fields $\{\Phi_0^T, \Phi_0^S\}$ transform as $(\mathbf{3}, 0)$ and $(\mathbf{3}, -2X_1)$, η_0 transforms as $(\mathbf{2}'', 0)$, and $\{\Theta_0, \Psi_0\}$ transform as $(\mathbf{1}, -2X_1)$ and $(\mathbf{1}, 0)$, respectively. For vacuum stability and the desired vacuum alignment solution, the flavon fields $\{\Phi_T, \eta\}$ are enforced to be neutral under $U(1)_X$. In addition, the superpotential W in the theory is uniquely determined by the $U(1)_R$ symmetry containing the usual R parity as a subgroup: $\{\text{matter fields} \rightarrow e^{i\xi/2} \text{matter fields}\}$ and $\{\text{driving fields} \rightarrow e^{i\xi} \text{driving fields}\}$,

³For some recent studies of flavored axions, see Refs. [1,8,17,19].

⁴It is likely that an exact continuous global symmetry is violated by quantum-gravitational effects [23].

with $W \rightarrow e^{i\xi}W$, whereas the flavon and Higgs fields remain invariant under a $U(1)_R$ symmetry. As in Ref. [17], the global minima of the potential are given at leading order by

$$\begin{aligned} \langle \Phi_T \rangle &= \frac{v_T}{\sqrt{2}}(1, 0, 0), \quad \langle \Phi_S \rangle = \frac{v_S}{\sqrt{2}}(1, 1, 1), \quad \langle \eta \rangle = \frac{v_\eta}{\sqrt{2}}(1, 0), \\ \langle \Psi \rangle &= \langle \tilde{\Psi} \rangle = \frac{v_\Psi}{\sqrt{2}}, \quad \langle \Theta \rangle = \frac{v_\Theta}{\sqrt{2}}, \quad \langle \tilde{\Theta} \rangle = 0, \end{aligned} \quad (2)$$

where $v_\Psi = v_{\tilde{\Psi}}$ and $\kappa = v_S/v_\Theta$ in the supersymmetry (SUSY) limit. The complex scalar fields are decomposed as follows [17]:

$$\begin{aligned} \Phi_{S_i} &= \frac{e^{i\phi_S}}{\sqrt{2}}(v_S + h_S), & \Theta &= \frac{e^{i\phi_\Theta}}{\sqrt{2}}(v_\Theta + h_\Theta), \\ \Psi &= \frac{v_\Psi}{\sqrt{2}}e^{i\frac{\phi_\Psi}{v_g}}\left(1 + \frac{h_\Psi}{v_g}\right), & \tilde{\Psi} &= \frac{v_{\tilde{\Psi}}}{\sqrt{2}}e^{-i\frac{\phi_{\tilde{\Psi}}}{v_g}}\left(1 + \frac{h_{\tilde{\Psi}}}{v_g}\right), \end{aligned} \quad (3)$$

in which $\Phi_{S1} = \Phi_{S2} = \Phi_{S3} \equiv \Phi_{S_i}$ and $h_\Psi = h_{\tilde{\Psi}}$ in the SUSY limit, and $v_g = \sqrt{v_{\tilde{\Psi}}^2 + v_\Psi^2}$. The NG modes A_1 and A_2 are expressed as

$$A_1 = \frac{v_S\phi_S + v_\Theta\phi_\Theta}{\sqrt{v_S^2 + v_\Theta^2}}, \quad A_2 = \phi_\Psi, \quad (4)$$

with the angular fields ϕ_S , ϕ_Θ , and ϕ_Ψ .

B. Quarks, leptons, and flavored axions

Under $SL_2(F_3) \times U(1)_X$ with $U(1)_R = +1$, the SM quark matter fields are comprised of the five (among seven) inequivalent representations $\mathbf{1}$, $\mathbf{1}'$, $\mathbf{1}''$, $\mathbf{2}'$, and $\mathbf{3}$ of $SL_2(F_3)$, and their assignments are shown in Tables I and II. Because of the chiral structure of weak interactions, bare fermion masses are not allowed in the SM. Fermion

TABLE I. Representations of the quark fields under $SL_2(F_3) \times U(1)_X$ with $U(1)_R = +1$.

Field	Q_1, Q_2, Q_3	\mathcal{D}^c, b^c	U^c, t^c
$SL_2(F_3)$	$\mathbf{1}, \mathbf{1}', \mathbf{1}''$	$\mathbf{2}', \mathbf{1}'$	$\mathbf{2}', \mathbf{1}'$
$U(1)_X$	$10p - 4q, 8p - 2q, 0$	$3q - 8p, 3q$	$-8p, 0$

TABLE II. Representations of the lepton fields under $SL_2(F_3) \times U(1)_X$ with $U(1)_R = +1$, with $r \equiv Q_{y_e} + p$.

Field	L	e^c, μ^c, τ^c	N^c	S_e^c, S_μ^c, S_τ^c
$SL_2(F_3)$	$\mathbf{3}$	$\mathbf{1}, \mathbf{1}'', \mathbf{1}'$	$\mathbf{3}$	$\mathbf{1}, \mathbf{1}'', \mathbf{1}'$
$U(1)_X$	$-r$	$r - Q_{y_e}, r - Q_{y_\mu},$ $r - Q_{y_\tau}$	p	$r - Q_{y_1^c}, r - Q_{y_2^c},$ $r - Q_{y_3^c}$

masses arise through Yukawa interactions [24]. Then the Yukawa superpotential for the quark-sector invariant under $G_{SM} \times G_F \times U(1)_R$ is written as

$$\begin{aligned} W_q^u &= \hat{y}_t t^c Q_3 H_u + y_c (\eta \mathcal{U}^c)_{1''} Q_2 \frac{H_u}{\Lambda} \\ &+ \tilde{y}_c [(\eta \mathcal{U}^c)_3 \Phi_T]_{1''} Q_2 \frac{H_u}{\Lambda^2} + y_u [(\eta \mathcal{U}^c)_3 \Phi_T]_1 Q_1 \frac{H_u}{\Lambda^2} \\ &+ \tilde{y}_u [(\eta \mathcal{U}^c)_3 \eta \eta]_1 Q_1 \frac{H_u}{\Lambda^3}, \end{aligned} \quad (5)$$

$$\begin{aligned} W_q^d &= y_b b^c Q_3 H_d + y_s (\eta \mathcal{D}^c)_{1''} Q_2 \frac{H_d}{\Lambda} \\ &+ Y_s b^c Q_2 (\Phi_S \Phi_S)_{1'} \frac{H_d}{\Lambda^2} + y_d [(\eta \mathcal{D}^c)_3 \Phi_S]_1 Q_1 \frac{H_d}{\Lambda^2} \\ &+ Y_d b^c Q_1 (\Phi_S \Phi_S)_{1''} \frac{H_d}{\Lambda^2} + \tilde{y}_d [(\eta \mathcal{D}^c)_3 \Phi_T]_1 Q_1 \frac{H_d}{\Lambda^2}. \end{aligned} \quad (6)$$

According to the assignment of the $U(1)_X$ quantum numbers to the matter field contents as in Table I, the Yukawa couplings of quark fermions are visualized as a function of the SM gauge-singlet flavon fields $\Psi(\tilde{\Psi})$ and/or $\Theta(\Phi_S)$, except for the top Yukawa coupling:

$$\begin{aligned} y_c &= \hat{y}_c \left(\frac{\tilde{\Psi}}{\Lambda}\right)^2, & \tilde{y}_c &= \hat{y}_c \left(\frac{\tilde{\Psi}}{\Lambda}\right)^2, \\ y_u &= \hat{y}_u \left(\frac{\tilde{\Psi}}{\Lambda}\right)^4 \frac{\Theta}{\Lambda}, & \tilde{y}_u &= \hat{y}_u \left(\frac{\tilde{\Psi}}{\Lambda}\right)^4 \frac{\Theta}{\Lambda}, \\ y_b &= \hat{y}_b \left(\frac{\Psi}{\Lambda}\right)^3, & y_s &= \hat{y}_s \left(\frac{\Psi}{\Lambda}\right), \\ y_d &= \hat{y}_d \left(\frac{\tilde{\Psi}}{\Lambda}\right), & \tilde{y}_d &= \hat{y}_d \left(\frac{\tilde{\Psi}}{\Lambda}\right) \frac{\Theta}{\Lambda}, \\ Y_s &= \hat{Y}_{s1} \left(\frac{\Theta}{\Lambda}\right)^2 \frac{\Psi}{\Lambda} + \hat{Y}_{s2} \left(\frac{\Phi_S}{\Lambda}\right)^2 \frac{\Psi}{\Lambda}, \\ Y_d &= \hat{Y}_{d1} \left(\frac{\Theta}{\Lambda}\right)^3 \frac{\tilde{\Psi}}{\Lambda} + \hat{Y}_{d2} \left(\frac{\Phi_S}{\Lambda}\right)^2 \frac{\Theta \tilde{\Psi}}{\Lambda}, \end{aligned} \quad (7)$$

where we recall that the ‘‘hat’’ Yukawa couplings are of order unity. The up-type quark superpotential in Eq. (5) does not contribute to the Cabibbo-Kobayashi-Maskawa (CKM) matrix due to the diagonal form of the mass matrix, while the down-type quark superpotential in Eq. (6) does contribute to the CKM matrix.

As discussed in Refs. [1,8,17], with the condition of $U(1)_X$ -[gravity]² anomaly cancellation new additional Majorana fermions $S_{e,\mu,\tau}^c$ besides the heavy Majorana neutrinos can be introduced in the lepton sector. Hence, such new additional Majorana neutrinos can play the role of active neutrinos as pseudo-Dirac neutrinos. Under $SL_2(F_3) \times U(1)_X$ with $U(1)_R = +1$, the quantum numbers of the lepton fields are summarized in Table II. The lepton Yukawa superpotential (similar to the quark

sector) invariant under $G_{\text{SM}} \times G_F \times U(1)_R$ reads at leading order

$$W_\ell = y_\tau \tau^c (L\Phi_T)_{1'} \frac{H_d}{\Lambda} + y_\mu \mu^c (L\Phi_T)_{1'} \frac{H_d}{\Lambda} + y_e e^c (L\Phi_T)_1 \frac{H_d}{\Lambda}, \quad (8)$$

$$W_\nu = y_3^s S_\tau^c (L\Phi_T)_{1'} \frac{H_u}{\Lambda} + y_2^s S_\mu^c (L\Phi_T)_{1'} \frac{H_u}{\Lambda} + y_1^s S_e^c (L\Phi_T)_1 \frac{H_u}{\Lambda} + y_\nu (LN^c)_1 H_u + \frac{1}{2} (\hat{y}_\Theta \Theta + \hat{y}_{\tilde{\Theta}} \tilde{\Theta}) (N^c N^c)_1 + \frac{\hat{y}_R}{2} (N^c N^c)_3 \Phi_S + \frac{1}{2} \{y_1^{ss} S_e^c S_e^c + y_2^{ss} S_\mu^c S_\mu^c + y_3^{ss} S_\tau^c S_\tau^c\} \Theta. \quad (9)$$

Below the cutoff scale Λ , the mass term of the Majorana neutrinos N^c comprises an exact tribimaximal mixing (TBM) pattern [25,26]. With the desired VEV alignment in Eq. (2), it is expected that the leptonic Pontecorvo-Maki-Nakagawa-Sakata mixing matrix at leading order is exactly compatible with a TBM,

$$\theta_{13} = 0, \quad \theta_{23} = \frac{\pi}{4} = 45^\circ, \quad \theta_{12} = \sin^{-1} \left(\frac{1}{\sqrt{3}} \right) \simeq 35.3^\circ. \quad (10)$$

In order to explain the present terrestrial neutrino oscillation data, nontrivial next-to-leading-order corrections should be taken into account, such as $(N^c N^c \Theta \Phi_T)_1 / \Lambda$, $(N^c N^c \Phi_S \Phi_T)_1 / \Lambda$, and $(LN^c \Phi_T)_1 H_u / \Lambda$. (We will consider neutrino phenomenology in detail in a future publication. See also the interesting paper Ref. [27].)

Here the $U(1)_X$ quantum numbers associated to the charged leptons are assigned in such a way that i) the charged lepton mass spectra are described and ii) the ratio of the electromagnetic $U(1)_X$ - $[U(1)_{\text{EM}}]^2$ and color anomaly $U(1)_X$ - $[SU(3)_C]^2$ coefficients lies in the range⁵ $0 < E/N < 4$, where $E = \sum_f (\delta_2^G X_{1f} + \delta_1^G X_{2f}) (Q_f^{\text{em}})^2$ and $N = 2\delta_1^G \delta_2^G$:

$$\frac{E}{N} = \frac{23}{6}, \quad \text{for } \mathcal{Q}_{y_\tau} = -3q, \quad \mathcal{Q}_{y_\mu} = -6q, \quad \mathcal{Q}_{y_e} = 11q \quad (\text{Case I}), \quad (11)$$

$$\frac{E}{N} = \frac{1}{2}, \quad \text{for } \mathcal{Q}_{y_\tau} = 3q, \quad \mathcal{Q}_{y_\mu} = 6q, \quad \mathcal{Q}_{y_e} = -11q \quad (\text{Case II}), \quad (12)$$

⁵This range is derived from the bound from the ADMX experiment [13], $(g_{\text{A}\gamma\gamma}/m_a)^2 \leq 1.44 \times 10^{-19} \text{ GeV}^{-2} \text{ eV}^{-2}$.

$$\frac{E}{N} = \frac{5}{2}, \quad \text{for } \mathcal{Q}_{y_\tau} = 3q, \quad \mathcal{Q}_{y_\mu} = 6q, \quad \mathcal{Q}_{y_e} = -11q \quad (\text{Case III}). \quad (13)$$

Similarly, the $U(1)_X$ quantum numbers associated to the neutrinos can be assigned by the anomaly-free condition of $U(1)_X$ - $[\text{gravity}]^2$ together with the measured active neutrino observables:

$$U(1)_X \times [\text{gravity}]^2 \propto 3\{4p - 3q\}_{\text{quark}} + \{3p - \mathcal{Q}_{y_1^s} - \mathcal{Q}_{y_2^s} - \mathcal{Q}_{y_3^s} - \mathcal{Q}_{y_e} - \mathcal{Q}_{y_\mu} - \mathcal{Q}_{y_\tau}\}_{\text{lepton}} = 0. \quad (14)$$

This vanishing anomaly, however, does not restrict \mathcal{Q}_{y_ν} (or equivalently $\mathcal{Q}_{y_i^s}$), whose quantum numbers can be constrained by the new astronomical-scale baseline neutrino oscillations, as shown in Refs. [1,17,28]. With the above $U(1)_X$ quantum numbers, such a $U(1)_X \times [\text{gravity}]^2$ anomaly is free for

$$21 \frac{X_1}{2} = k_2 X_2 \quad \text{with} \quad k_2 = \left\{ \begin{array}{l} 11 - \tilde{\mathcal{Q}}_{y_1^s} - \tilde{\mathcal{Q}}_{y_2^s} - \tilde{\mathcal{Q}}_{y_3^s} \quad (\text{Case I}) \\ 1 - \tilde{\mathcal{Q}}_{y_1^s} - \tilde{\mathcal{Q}}_{y_2^s} - \tilde{\mathcal{Q}}_{y_3^s} \quad (\text{Case II}) \\ 7 - \tilde{\mathcal{Q}}_{y_1^s} - \tilde{\mathcal{Q}}_{y_2^s} - \tilde{\mathcal{Q}}_{y_3^s} \quad (\text{Case III}) \end{array} \right\}, \quad (15)$$

where $\tilde{\mathcal{Q}}_{y_i^s} = \mathcal{Q}_{y_i^s}/X_2$. As in Refs. [1,17], we choose $k_2 = \pm 21$ for the $U(1)_{X_i}$ charges as they are the smallest values that avoid the axionic domain-wall problem. Hence, for Cases I, II, and III, $\tilde{\mathcal{Q}}_{y_1^s} + \tilde{\mathcal{Q}}_{y_2^s} + \tilde{\mathcal{Q}}_{y_3^s} = -10$ (32), -20 (22), and -14 (28), respectively, for $k_2 = 21(-21)$. Then, the color anomaly coefficients are given by $\delta_1^G = 2X_1$ and $\delta_2^G = -3X_2$, and subsequently the axionic domain-wall condition as in Ref. [17] is expressed with the reduced $k_1 = \pm k_2 = 1$ as $N_1 = 4$ and $N_2 = 3$. Clearly, in the QCD instanton backgrounds since N_1 and N_2 are relative primes there is no $Z_{N_{\text{DW}}}$ discrete symmetry, and therefore no axionic domain-wall problem occurs.

Once the scalar fields Φ_S , Θ , $\tilde{\Theta}$, Ψ , and $\tilde{\Psi}$ acquire VEVs, the flavor symmetry $U(1)_X \times SL_2(F_3)$ is spontaneously broken,⁶ and at energies below the electroweak scale all quarks and leptons obtain masses. The relevant Yukawa interaction terms with chiral fermions ψ charged under the flavored $U(1)_X$ symmetry is given by

⁶If the symmetry $U(1)_X$ is broken spontaneously, the massless modes A_1 of the scalar Φ_S (or Θ) and A_2 of the scalar Ψ ($\tilde{\Psi}$) appear as phases.

$$\begin{aligned}
-\mathcal{L}_{YW} = & \bar{q}_R^u \mathcal{M}_u q_L^u + \bar{q}_R^d \mathcal{M}_d q_L^d + \bar{\ell}_R \mathcal{M}_\ell \ell_L + \frac{g}{\sqrt{2}} W_\mu^+ \bar{q}_L^u \gamma^\mu q_L^d + \frac{g}{\sqrt{2}} W_\mu^- \bar{\ell}_L \gamma^\mu \nu_L \\
& + \frac{1}{2} \begin{pmatrix} \bar{\nu}_L^e & \bar{S}_R & \bar{N}_R \end{pmatrix} \begin{pmatrix} 0 & m_{DS}^T & m_D^T \\ m_{DS} & e^{i\frac{A_1}{v_F}} M_S & 0 \\ m_D & 0 & e^{i\frac{A_1}{v_F}} M_R \end{pmatrix} \begin{pmatrix} \nu_L \\ S_R^c \\ N_R^c \end{pmatrix} + \text{H.c.}, \quad (16)
\end{aligned}$$

where g is the $SU(2)$ coupling constant, $q^u = (u, c, t)$, $q^d = (d, s, b)$, $\ell = (e, \mu, \tau)$, and $\nu_L = (\nu_e, \nu_\mu, \nu_\tau)$.

1. Quarks, CKM mixings, and flavored axions

Now, let us discuss the realization of quark masses and mixings, in which the physical mass hierarchies are directly responsible for the assignment of $U(1)_X$ quantum numbers.

The axion coupling matrices to the up- and down-type quarks, respectively, are diagonalized through biunitary transformations, $V_R^\psi \mathcal{M}_\psi V_L^{\psi\dagger} = \hat{\mathcal{M}}_\psi$ (diagonal form), and the mass eigenstates $\psi'_R = V_R^\psi \psi_R$ and $\psi'_L = V_L^\psi \psi_L$. With the desired VEV directions in Eq. (2), in the above Lagrangian (16) the mass matrices \mathcal{M}_u and \mathcal{M}_d for up- and down-type quarks, respectively, are expressed as

$$\mathcal{M}_u = \begin{pmatrix} (iy_u \nabla_T - \tilde{y}_u \nabla_\eta^2) \nabla_\eta e^{i(\frac{A_1}{v_F} - 4\frac{A_2}{v_g})} & 0 & 0 \\ 0 & (y_c + \frac{1-i}{2} \tilde{y}_c \nabla_T) \nabla_\eta e^{-2i\frac{A_2}{v_g}} & 0 \\ 0 & 0 & \hat{y}_t \end{pmatrix} v_u, \quad (17)$$

$$\mathcal{M}_d = \begin{pmatrix} (iy_d \nabla_S + \tilde{y}_d \nabla_T) \nabla_\eta e^{i(\frac{A_1}{v_F} - \frac{A_2}{v_g})} & 0 & 0 \\ \frac{1-i}{2} y_d \nabla_\eta \nabla_S e^{i(\frac{A_1}{v_F} - \frac{A_2}{v_g})} & y_s \nabla_\eta e^{\frac{A_2}{v_g}} & 0 \\ 3Y_d \nabla_S^2 e^{i(5\frac{A_1}{v_F} - \frac{A_2}{v_g})} & 3Y_s \nabla_S^2 e^{i(4\frac{A_1}{v_F} + \frac{A_2}{v_g})} & y_b e^{3i\frac{A_2}{v_g}} \end{pmatrix} v_d, \quad (18)$$

where $v_d \equiv \langle H_d \rangle = v \cos \beta / \sqrt{2}$ and $v_u \equiv \langle H_u \rangle = v \sin \beta / \sqrt{2}$ with $v \simeq 246$ GeV, and

$$\nabla_Q \equiv \frac{v_Q}{\sqrt{2}\Lambda} \quad \text{with} \quad Q = \eta, S, T, \Theta, \Psi, \tilde{\Psi}. \quad (19)$$

In the above mass matrices the corresponding Yukawa terms for up- and down-type quarks are given by

$$\begin{aligned}
y_u = \hat{y}_u \nabla_\Theta \nabla_{\tilde{\Psi}}^4, & \quad \tilde{y}_u = \hat{\tilde{y}}_u \nabla_\Theta \nabla_{\tilde{\Psi}}^4, & y_c = \hat{y}_c \nabla_\Psi^2, & \quad \tilde{y}_c = \hat{\tilde{y}}_c \nabla_\Psi^2, \\
y_d = \hat{y}_d \nabla_{\tilde{\Psi}}, & \quad \tilde{y}_d = \hat{\tilde{y}}_d \nabla_{\tilde{\Psi}} \nabla_\Theta, & y_s = \hat{y}_s \nabla_\Psi, & \quad y_b = \hat{y}_b \nabla_{\tilde{\Psi}}^3.
\end{aligned} \quad (20)$$

Due to the diagonal form of the up-type quark mass matrix in Eq. (36), the CKM mixing matrix $V_{\text{CKM}} \equiv V_L^u V_L^{d\dagger}$ coming from the charged quark-current term in Eq. (16) is generated from the down-type quark matrix in Eq. (18),

$$V_{\text{CKM}} = V_L^{d\dagger} = \begin{pmatrix} 1 - \frac{1}{2}\lambda^2 & \lambda & A\lambda^3(\rho + i\eta) \\ -\lambda & 1 - \frac{1}{2}\lambda^2 & A\lambda^2 \\ A\lambda^3(1 - \rho + i\eta) & -A\lambda^2 & 1 \end{pmatrix} + \mathcal{O}(\lambda^4), \quad (21)$$

in the Wolfenstein parametrization [29] and at higher precision [30], where $\lambda = 0.22509_{-0.00071}^{+0.00091}$, $A = 0.825_{-0.037}^{+0.020}$, $\bar{\rho} = \rho/(1 - \lambda^2/2) = 0.160_{-0.021}^{+0.034}$, and $\bar{\eta} = \eta/(1 - \lambda^2/2) = 0.350_{-0.024}^{+0.024}$ with 3σ errors [31].

The quark mass matrices \mathcal{M}_u in Eq. (17) and \mathcal{M}_d in Eq. (18) generate the up- and down-type quark masses:

$$\begin{aligned}\hat{\mathcal{M}}_u &= P_u^* \mathcal{M}_u Q_u = \text{diag}(m_u, m_c, m_t), \\ \hat{\mathcal{M}}_d &= V_R^{d\dagger} \mathcal{M}_d V_L^d = \text{diag}(m_d, m_s, m_b),\end{aligned}\quad (22)$$

$$\begin{aligned}\frac{m_d}{m_b} &\doteq 1.12_{-0.11}^{+0.13} \times 10^{-3}, & \frac{m_s}{m_b} &\doteq 2.30_{-0.12}^{+0.21} \times 10^{-2}, & \frac{m_u}{m_t} &\doteq 2.41_{-0.03}^{+0.03} \times 10^{-2}, \\ \frac{m_u}{m_d} &\doteq 0.38 - 0.58, & \frac{m_c}{m_t} &\doteq 7.39_{-0.20}^{+0.20} \times 10^{-3}, & \frac{m_u}{m_c} &\doteq 1.72_{-0.34}^{+0.52} \times 10^{-3},\end{aligned}\quad (23)$$

$$m_b = 4.18_{-0.03}^{+0.04} \text{ GeV}, \quad m_c = 1.28 \pm 0.03 \text{ GeV}, \quad m_t = 173.1 \pm 0.6 \text{ GeV},\quad (24)$$

where c - and b -quark masses are the running masses in the $\overline{\text{MS}}$ scheme, and the light u -, d -, and s -quark masses are the current quark masses in the $\overline{\text{MS}}$ scheme at the momentum scale $\mu \approx 2 \text{ GeV}$. So, the following new expansion parameters are defined such that the diagonalizing matrix V_L^d satisfies the CKM matrix as well as the empirical quark masses and their ratios in Eqs. (23) and (24):

$$\nabla_T = \kappa \frac{|\hat{y}_d|}{|\hat{y}_d|} \quad \text{with} \quad \phi_{\bar{d}} = -\phi_d - \frac{\pi}{2},\quad (25)$$

$$\nabla_{\Theta} = \frac{1}{\kappa} \nabla_S = \left| \frac{X_2 \delta_1^G}{X_1 \delta_2^G} \right| \sqrt{\frac{2}{1 + \kappa^2}} \nabla_{\Psi},\quad (26)$$

$$\nabla_{\eta} = \left(\frac{m_c}{m_t} \right)_{\text{PDG}} \left| \frac{\hat{y}_t}{\hat{y}_c + \hat{y}_c \nabla_T} \right| \frac{1}{\nabla_{\Psi}^2},\quad (27)$$

$$\nabla_{\Psi} \simeq \lambda \left| \frac{X_1 \delta_2^G}{X_2 \delta_1^G} \right|^{\frac{2}{3}} \left(\frac{B(1 + \kappa^2)}{6\kappa^2} \frac{|\hat{y}_b|}{|\hat{y}_{d1} + 3\kappa^2 \hat{y}_{d2}|} \right)^{\frac{1}{3}}.\quad (28)$$

Then, the mixing matrix $V_L^{d\dagger} = V_{\text{CKM}}$ is obtained by diagonalizing the Hermitian matrix $\mathcal{M}_d^{\dagger} \mathcal{M}_d$:

$$V_L^d \mathcal{M}_d^{\dagger} \mathcal{M}_d V_L^{d\dagger} = \text{diag}(|m_d|^2, |m_s|^2, |m_b|^2).\quad (29)$$

where P_u and Q_u are diagonal phase matrices, and V_L^d and V_R^d can be determined by diagonalizing the matrices for $\mathcal{M}_d^{\dagger} \mathcal{M}_d$ and $\mathcal{M}_d \mathcal{M}_d^{\dagger}$, respectively. The physical structures of the up- and down-type quark Lagrangians should match the empirical up- and down-type quark masses and their ratios calculated from the measured Particle Data Group (PDG) values [32]:

The CKM mixing angles in the standard parametrization [33] can be roughly described as

$$\begin{aligned}\theta_{12}^q &\simeq \frac{1}{\sqrt{2}} \left| \frac{\hat{y}_d}{\hat{y}_s} \right| \nabla_S, \\ \theta_{23}^q &\simeq 3\kappa^2 \left| \frac{\hat{Y}_{s1} + 3\kappa^2 \hat{Y}_{s2}}{\hat{y}_b} \right| \frac{\nabla_{\Theta}^4}{\nabla_{\Psi}^2}, \\ \theta_{13}^q &\simeq 3 \left| \frac{\hat{Y}_{d1} + 3\kappa^2 \hat{Y}_{d2}}{\hat{y}_b} \right| \nabla_{\Psi} \nabla_S^2.\end{aligned}\quad (30)$$

With the redefinition of the quark fields, the CKM CP phase is

$$\delta_{CP}^q \equiv \tan^{-1}(\eta/\rho) = \phi_2^d - 2\phi_3^d,\quad (31)$$

where $\phi_2^d \simeq \arg\{(\hat{Y}_{d1}^* + 3\kappa^2 \hat{Y}_{d2}^*) \hat{y}_b\}/2 - \phi_1^d/2$ and $2\phi_3^d \simeq \arg(\hat{y}_s \hat{y}_b) + \phi_1^d - \phi_2^d + \pi/4$, and $\phi_1^d = \arg\{(\hat{Y}_{s1}^* + 3\kappa^2 \hat{Y}_{s2}^*) \hat{y}_b\}/2$. As designed, the CKM matrix is well described with $J_{CP}^{\text{quark}} = \text{Im}[V_{us} V_{cb} V_{ub}^* V_{cs}^*] \simeq A^2 \lambda^6 \sqrt{\rho^2 + \eta^2} \sin \delta_{CP}^q$. Subsequently, the up- and down-type quark masses are obtained as

$$\begin{aligned}m_t &\simeq |\hat{y}_t| v_u, & m_b &\simeq |\hat{y}_b| |\nabla_{\Psi}^3| v_b, \\ m_c &\simeq \left| \hat{y}_c + \frac{1-i}{2} \hat{y}_c \nabla_T \right| \nabla_{\Psi}^2 \nabla_{\eta} v_u, & m_s &\simeq |\hat{y}_s| |\nabla_{\Psi} \nabla_{\eta}| v_d, \\ m_u &\simeq \nabla_{\Psi}^4 \nabla_{\eta} \nabla_{\Theta} |i \hat{y}_u \nabla_T - \hat{y}_u \nabla_{\eta}^2| v_u, & m_d &\simeq 2 |\hat{y}_d \sin \phi_d| |\nabla_{\Psi} \nabla_{\eta}| \nabla_S v_d,\end{aligned}\quad (32)$$

and the parameter of $\tan \beta \equiv v_u/v_d$ is given in terms of the PDG value in Eq. (24) by

$$\tan \beta \simeq \left(\frac{m_t}{m_b} \right)_{\text{PDG}} \left| \frac{\hat{y}_b}{\hat{y}_t} \right| \nabla_{\Psi}^3.\quad (33)$$

Since all of the parameters in the quark sector are correlated with one another, it is very crucial for obtaining the values of the new expansion parameters to reproduce the empirical results of the CKM mixing angles and quark masses. Moreover, since such parameters are also closely correlated with those in the lepton sector, finding the values of these parameters is crucial for producing the empirical results of the charged leptons [see below Eq. (36)] and the light active neutrino masses in our model.

2. Numerical analysis for quark masses and CKM mixing angles

We perform a numerical simulation⁷ using the linear algebra tools of Ref. [34]. With the inputs

$$\tan\beta = 4.7, \quad \kappa = 0.33, \quad (34)$$

and $|\hat{y}_d| = 1.1$ ($\phi_d = 3.070$ rad), $|\hat{y}_{d'}| = 1.194$, $|\hat{y}_s| = 0.370$ ($\phi_s = 4.920$ rad), $|\hat{y}_b| = 2.280$ ($\phi_b = 0$), $|\hat{y}_u| = 0.400$ ($\phi_u = 0$), $|\hat{y}_{u'}| = 1.0$ ($\phi_{u'} = 0$), $|\hat{y}_c| = 2.800$ ($\phi_c = 3.600$ rad), $|\hat{y}_{c'}| = 1.000$ ($\phi_{c'} = 0$), $|\hat{y}_t| = 1.017$ ($\phi_t = 0$), $|\hat{Y}_{d1}| = 0.900$ ($\phi_{Y_{d1}} = 4.800$ rad), $|\hat{Y}_{d2}| = 0.800$ ($\phi_{Y_{d2}} = 0$), $|\hat{Y}_{s1}| = 2.600$ ($\phi_{Y_{s1}} = 6.500$ rad), and $|\hat{Y}_{s2}| = 1.900$ ($\phi_{Y_{s2}} = 0.117$ rad), leading to

$$\nabla_\Psi = 0.370, \quad \nabla_S = 0.109, \quad \nabla_T = 0.304, \quad \nabla_\eta = 0.020, \quad (35)$$

we obtain the mixing angles and Dirac CP phase $\theta_{12}^q = 12.98^\circ$, $\theta_{23}^q = 2.32^\circ$, $\theta_{13}^q = 0.22^\circ$, $\delta_{CP}^q = 65.18^\circ$ compatible with the 3σ global fit of CKMfitter [31]; the quark masses $m_d = 4.49$ MeV, $m_s = 101.62$ MeV, $m_b = 4.18$ GeV, $m_u = 2.57$ MeV, $m_c = 1.28$ GeV, and $m_t = 173.1$ GeV are compatible with the PDG values [32].

3. Charged leptons and flavored axions

According to the $U(1)_X$ charge assignment of the charged-leptons in Eqs. (11)–(13), the charged-lepton mass matrix in the Lagrangian (16) is written as

$$\mathcal{M}_\ell = \begin{pmatrix} y_e e^{\frac{Q_e A_2}{v_g}} & 0 & 0 \\ 0 & y_\mu e^{\frac{Q_\mu A_2}{v_g}} & 0 \\ 0 & 0 & y_\tau e^{\frac{Q_\tau A_2}{v_g}} \end{pmatrix} v_d, \quad (36)$$

where $Q_e = -11$, $Q_\mu = 6$, $Q_\tau = 3$ for Case I ($E/N = 23/6$), $Q_e = 11$, $Q_\mu = -6$, $Q_\tau = -3$ for the Case II ($E/N = 1/2$),

and $Q_e = 11$, $Q_\mu = -6$, $Q_\tau = -3$ for the Case III ($E/N = 5/2$). The corresponding Yukawa terms are expressed in terms of Eqs. (19) and (28) used in the quark sector as

$$y_e = \hat{y}_e \nabla_\Psi^{11}, \quad y_\mu = \hat{y}_\mu \nabla_\Psi^6, \quad y_\tau = \hat{y}_\tau \nabla_\Psi^3, \quad (37)$$

where $\nabla_\Psi = \nabla_{\hat{\Psi}}$ in the SUSY limit is used. The ‘‘hat’’ Yukawa couplings $\hat{y}_{e,\mu,\tau}$ are fixed⁸ as $\hat{y}_e = 0.793152$, $\hat{y}_\mu = 1.137250$, and $\hat{y}_\tau = 0.968747$ by using the numerical values of Eq. (35) in the quark sector via the empirical results $m_e = 0.511$ MeV, $m_\mu = 105.683$ MeV, and $m_\tau = 1776.86$ MeV [32].

III. SCALE OF THE PQ PHASE TRANSITION AND QCD AXION PROPERTIES

The couplings of the flavored axions and the mass of the QCD axion are inversely proportional to the PQ symmetry breaking scale. In the theoretical view of Refs. [1,8,17], the scale of PQ symmetry breakdown congruent to that of the seesaw mechanism can push the scale far beyond the electroweak scale, rendering the flavored axions very weakly interacting particles. Since the weakly coupled flavored axions (one linear combination of the QCD axion and its orthogonal ALP) could carry away a large amount of energy from the interior of stars, according to the standard stellar evolution scenario their couplings should be bounded with electrons,⁹ photons, and nucleons. Hence, such weakly coupled flavored axions have a wealth of interesting phenomenological implications in the context of astroparticle physics [1,17], like the formation of a cosmic diffuse background of axions from the Sun [35,36], from evolved low-mass stars such as red giants and horizontal-branch stars in globular clusters [37,38] or white dwarfs [39,40], from neutron stars [41], and from the duration of the neutrino burst of the core-collapse supernova SN1987A [42] as well as the rare flavor-changing decay processes induced by the flavored axions $K^+ \rightarrow \pi^+ + A_i$ [16,43] and $\mu \rightarrow e + \gamma + A_i$ [43,44].

Such flavored axions could be produced in hot astrophysical plasmas, thus transporting energy out of stars and other astrophysical objects, and they could also be produced by the rare flavor-changing decay processes. Actually, the coupling strengths of these particles with normal matter and radiation are bounded by the constraint that stellar lifetimes and energy-loss rates [45] as well as the branching ratios for the μ and K flavor-changing decays [16,44] should agree with observations. Interestingly enough, recent observations also show a preference for extra energy losses in stars at different evolutionary

⁷Here, in our numerical calculation, we only consider the mass matrices in Eqs. (17) and (18) since it is expected that the corrections to the VEVs due to higher-dimensional operators are below the few-percent level.

⁸The charged-lepton sector (like the quark sector) has VEV corrections and the ‘‘hat’’ Yukawa couplings are corrected.

⁹The second (μ) and third (τ) generation particles are absent in almost all astrophysical objects.

stages: red giants, supergiants, helium-core-burning stars, white dwarfs, and neutron stars (see Ref. [14] for a summary of extra cooling observations and Ref. [1] for an interpretation of the bound of the QCD axion decay constant); the present experimental limit, $\text{Br}(K^+ \rightarrow \pi^+ A_i) < 7.3 \times 10^{-11}$ [16], puts a lower bound on the axion decay constant, and in the near future the NA62 experiment [expected to reach a sensitivity of $\text{Br}(K^+ \rightarrow \pi^+ A_i) < 1.0 \times 10^{-12}$ [46]] will probe the flavored axions or put a severe bound on the QCD axion decay constant F_A (or flavored axion decay constants $F_{a_i} = f_{a_i}/\delta_i^G$). According to the recent investigation in Refs. [1,17], the flavored axions (the QCD axion and its orthogonal ALP) would provide very good hints for a new physics model for quarks and leptons. Fortunately, in the framework of flavored-PQ symmetry the cooling anomalies hint at axion couplings to electrons, photons, and neutrons, which should not conflict with the current upper bound on the rare $K^+ \rightarrow \pi^+ A_i$ decay. We note that once the scale of PQ symmetry breakdown is fixed the other values are automatically, including the QCD axion decay constant and the mass scale of heavy neutrinos associated with the seesaw mechanism.

In order to fix the QCD axion decay constant F_A (or flavored axion decay constants $F_{a_i} = f_{a_i}/\delta_i^G$), we will consider two tight constraints coming from astroparticle physics: axion cooling of stars via bremsstrahlung off electrons, and flavor-violating processes induced by the flavored axions.

A. Flavored-axion cooling of stars via bremsstrahlung off electrons

In the present model, since the flavored axion A_2 couples directly to electrons, the axion can be emitted by Compton scattering, atomic axio-recombination and axio-deexcitation, and axio-bremsstrahlung in electron-ion or electron-electron collisions [37]. The flavored axion A_2 coupling to electrons in the model reads

$$g_{\text{Aee}} = \frac{X_e m_e}{\sqrt{2} \delta_2^G F_A}, \quad (38)$$

where $m_e = 0.511$ MeV, $F_A = f_{a_i}/\sqrt{2} \delta_i^G$, $\delta_2^G = -3X_2$, and $X_e = -11X_2$. Indeed, the longstanding anomaly in the cooling of white dwarfs and red-giant-branch stars in globular clusters where bremsstrahlung off electrons is mainly efficient [39] could be explained by axions with the fine-structure constant of the axion to electrons, $\alpha_{\text{Aee}} = (0.29 - 2.30) \times 10^{-27}$ [47] and $\alpha_{\text{Aee}} = (0.41 - 3.70) \times 10^{-27}$ [40,48], indicating the clear systematic tendency of stars to cool faster than predicted. As recently reexamined in Ref. [14], Eq. (1) with $\alpha_{\text{Aee}} = g_{\text{Aee}}^2/4\pi$ is interpreted in terms of the QCD axion decay constant in the present model as

$$0.5 \times 10^{10} \lesssim F_A [\text{GeV}] \lesssim 4.4 \times 10^{10}. \quad (39)$$

This bound comes from the $U(1)_X$ quantum number of the electron, $X_e = -11X_2$, as shown in Eq. (36). Note that the $U(1)_X$ quantum number of charged leptons in Eqs. (11)–(13) is different from the one in Ref. [17] because of the different flavor structures of Yukawa interactions [see Eqs. (17), (18), and (36)], leading to the different values of the expansion parameters (34) and (35) satisfying the empirical quark and lepton masses and mixings.

B. Flavor-changing process $K^+ \rightarrow \pi^+ + A_i$ induced by the flavored axions

Below the QCD scale ($1 \text{ GeV} \approx 4\pi f_\pi$), the chiral symmetry is broken and π , K , and η are produced as pseudo-Goldstone bosons. Since a direct interaction of the SM gauge-singlet flavon fields charged under $U(1)_X$ with the SM quarks charged under $U(1)_X$ can arise through Yukawa interactions, the flavor-changing process $K^+ \rightarrow \pi^+ + A_i$ is induced by the flavored axions A_i . Then, the flavored-axion interactions with the flavor-violating coupling to the s and d quarks is given by

$$\mathcal{L}_Y^{A_i s d} \simeq i \left(\frac{|X_1| |A_1|}{2f_{a_1}} - \frac{|X_2| |A_2|}{f_{a_2}} \right) \bar{s} d (m_s - m_d) \lambda \left(1 - \frac{\lambda^2}{2} \right), \quad (40)$$

where¹⁰ $V_L^{d\dagger} = V_{\text{CKM}}$, $f_{a_1} = |X_1| v_\Theta (1 + \kappa^2)^{1/2}$, and $f_{a_2} = |X_2| v_g$ are used. Then, the decay width of $K^+ \rightarrow \pi^+ + A_i$ is given by [43,49]

$$\Gamma(K^+ \rightarrow \pi^+ + A_i) = \frac{m_K^3}{16\pi} \left(1 - \frac{m_\pi^2}{m_K^2} \right)^3 |\mathcal{M}_{dsi}|^2, \quad (41)$$

where $m_{K^\pm} = 493.677 \pm 0.013$ MeV, $m_{\pi^\pm} = 139.57018(35)$ MeV [32], and

$$\begin{aligned} |\mathcal{M}_{ds1}|^2 &= \left| \frac{X_1}{2\sqrt{2}\delta_1^G F_A} \lambda \left(1 - \frac{\lambda^2}{2} \right) \right|^2, \\ |\mathcal{M}_{ds2}|^2 &= \left| \frac{X_2}{\sqrt{2}\delta_2^G F_A} \lambda \left(1 - \frac{\lambda^2}{2} \right) \right|^2, \end{aligned} \quad (42)$$

where $F_A = f_{a_i}/(\delta_i^G \sqrt{2})$ is used. From the present experimental upper bound in Eq. (1), $\text{Br}(K^+ \rightarrow \pi^+ A_i) < 7.3 \times 10^{-11}$, with $\text{Br}(K^+ \rightarrow \pi^+ \nu \bar{\nu}) = 1.73_{-1.05}^{+1.15} \times 10^{-10}$ [50], we obtain the lower limit on the QCD axion decay constant,

¹⁰In the standard parametrization, the mixing elements of V_R^d are given by $\theta_{23}^R \simeq A\lambda^2 (\nabla_\eta/\kappa^2 \nabla_\Psi^2) |\hat{y}_s/\hat{y}_b|$, $\theta_{13}^R \simeq AB\lambda^5 |\sin \phi_d| |\hat{y}_d/(\hat{Y}_{s1} + 3\kappa^2 \hat{Y}_{s2})| (2\nabla_\eta/3\kappa \nabla_\Psi^3)$, and $\theta_{12}^R \simeq 2\sqrt{2} |\sin \phi_d| \lambda^2$. Its effect on the flavor-violating coupling to the s and d quarks is negligible: $(V_R^d \text{Diag}(-4\frac{A_1}{v_F}, -4\frac{A_1}{v_F}, 0) V_R^{d\dagger})_{12} = 0$ at leading order.

$$F_A \gtrsim 2.72 \times 10^{10} \text{ GeV}. \quad (43)$$

Hence, from Eqs. (39) and (43) we can obtain the strongest bound on the QCD axion decay constant,

$$F_A = 3.56_{-0.84}^{+0.84} \times 10^{10} \text{ GeV}. \quad (44)$$

Interestingly enough, from Eqs. (35) and (44) the scale $\Lambda = 3F_A/(\sqrt{2}\nabla_\psi)$ responsible for the FN mechanism can be determined,

$$\Lambda = 2.04_{-0.48}^{+0.48} \times 10^{11} \text{ GeV}. \quad (45)$$

The NA62 experiment is expected to reach a sensitivity of $\text{Br}(K^+ \rightarrow \pi^+ + A_i) < 1.0 \times 10^{-12}$ in the near future [46], which is interpreted as the flavored axion decay constant and its corresponding QCD axion decay constant,

$$f_{a_i} > 9.86 \times 10^{11} \text{ GeV} \Leftrightarrow F_A > 2.32 \times 10^{11} \text{ GeV}. \quad (46)$$

Clearly, the NA62 experiment will probe the flavored axions or exclude the present model.

C. QCD axion interactions with nucleons

Below the chiral symmetry breaking scale, the axion-hadron interactions are meaningful (rather than the axion-quark interactions) for the axion production rate in the core of a star where the temperature is not as high as 1 GeV, which is given by [8]

$$-\mathcal{L}^{a-\psi_N} = \frac{\partial_\mu a}{2F_A} X_{\psi_N} \bar{\psi}_N \gamma_\mu \gamma^5 \psi_N, \quad (47)$$

where a is the QCD axion, its decay constant is given by $F_A = f_A/N$ with $f_A = \sqrt{2}\delta_2^G f_{a_1} = \sqrt{2}\delta_1^G f_{a_2}$, and ψ_N is the nucleon doublet $(p, n)^T$ (here p and n correspond to the proton field and neutron field, respectively). Recently, the couplings of the axion to the nucleon were extracted at high precision [51]:

$$X_p = -0.47(3) + 0.88(3) \frac{\tilde{X}_u}{N} - 0.39(2) \frac{\tilde{X}_d}{N} - 0.038(5) \frac{\tilde{X}_s}{N} - 0.012(5) \frac{\tilde{X}_c}{N} - 0.009(2) \frac{\tilde{X}_b}{N} - 0.0035(4) \frac{\tilde{X}_t}{N}, \quad (48)$$

$$X_n = -0.02(3) + 0.88(3) \frac{\tilde{X}_d}{N} - 0.39(2) \frac{\tilde{X}_u}{N} - 0.038(5) \frac{\tilde{X}_s}{N} - 0.012(5) \frac{\tilde{X}_c}{N} - 0.009(2) \frac{\tilde{X}_b}{N} - 0.0035(4) \frac{\tilde{X}_t}{N}, \quad (49)$$

where $N = 2\delta_1^G \delta_2^G$ with $\delta_1^G = 2X_1$ and $\delta_2^G = -3X_2$, and $\tilde{X}_q = \delta_2^G X_{1q} + \delta_1^G X_{2q}$ with $q = u, d, s$ and $X_{1u} = X_1$, $X_{1d} = X_1$, $X_{1s} = 0$, $X_{1c} = 0$, $X_{1b} = 0$, $X_{1t} = 0$, $X_{2u} = -4X_2$, $X_{2d} = -X_2$, $X_{2s} = X_2$, $X_{2c} = -2X_2$,

$X_{2b} = 3X_2$, and $X_{2t} = 0$. The QCD axion coupling to the neutron is written as

$$g_{\text{Ann}} = \frac{|X_n| m_n}{F_A}, \quad (50)$$

where the neutron mass $m_n = 939.6$ MeV. The state-of-the-art upper limit on this coupling, $g_{\text{Ann}} < 8 \times 10^{-10}$ [52], from neutron star cooling is interpreted as the lower bound of the QCD axion decay constant,

$$F_A > 9.53 \times 10^7 \text{ GeV}. \quad (51)$$

Clearly, the strongest bound on the QCD axion decay constant comes from the flavored-axion cooling of stars via bremsstrahlung off electrons in Eq. (39) as well as the flavor-changing process $K^+ \rightarrow \pi^+ + A_i$ induced by the flavored axions in Eq. (43).

Using the state-of-the-art calculation in Eq. (49) and the QCD axion decay constant in Eq. (44), we obtain

$$g_{\text{Ann}} = 2.14_{-0.41}^{+0.66} \times 10^{-12}, \quad (52)$$

which is *incompatible* with the hint for extra cooling from the neutron star in the supernova remnant Cassiopeia A by axion neutron bremsstrahlung, $g_{\text{Ann}} = 3.74_{-0.74}^{+0.62} \times 10^{-10}$ [53]. This huge discrepancy may be explained by considering other mechanisms for the cooling of the superfluid core of a neutron star, such as by neutrino-pair emission in a multicomponent superfluid state, ${}^3\text{P}_2(m_j = 0, \pm 1, \pm 2)$ [54].

D. QCD axion mass and its interactions with photons

With the well-constrained QCD axion decay constant in Eq. (44) congruent to the seesaw scale, we can predict the QCD axion mass and its corresponding axion-photon coupling.

As in Refs. [1,8], the axion mass in terms of the pion mass and pion decay constant is obtained as

$$m_a^2 F_A^2 = m_{\pi^0}^2 f_\pi^2 F(z, w), \quad (53)$$

where¹¹ $f_\pi = 92.21(14)$ MeV [32] and

$$F(z, w) = \frac{z}{(1+z)(1+z+w)} \quad \text{with} \\ z \equiv \frac{m_u^{\text{MS}}(2 \text{ GeV})}{m_d^{\text{MS}}(2 \text{ GeV})} = 0.48(3) \quad \text{and} \\ \omega = 0.315z. \quad (54)$$

¹¹As in Ref. [51], here $F(z, \omega)$ can be replaced to high accuracy by $F(z) = \frac{z}{(1+z)^2} \{1 + 2 \frac{m_s^0}{f_\pi^2} (h_r + \frac{z^2 - 6z + 1}{(1+z)^2} l_r)\}$, where $h_r = (4.8 \pm 1.4) \times 10^{-3}$ and $l_r = 7(4) \times 10^{-3}$.

Note that the Weinberg value lies in the range $0.38 < z < 0.58$ [32,55]. After integrating out the heavy π^0 and η at low energies, there is an effective low-energy Lagrangian with an axion-photon coupling $g_{a\gamma\gamma}$:

$$\mathcal{L}_{a\gamma\gamma} = \frac{1}{4} g_{a\gamma\gamma} a_{\text{phys}} F^{\mu\nu} \tilde{F}_{\mu\nu} = -g_{a\gamma\gamma} a_{\text{phys}} \vec{E} \cdot \vec{B}, \quad (55)$$

where \vec{E} and \vec{B} are the electromagnetic field components. The axion-photon coupling can be expressed in terms of

the QCD axion mass, pion mass, pion decay constant, z , and w :

$$g_{a\gamma\gamma} = \frac{\alpha_{\text{em}}}{2\pi} \frac{m_a}{f_\pi m_{\pi^0}} \frac{1}{\sqrt{F(z, w)}} \left(\frac{E}{N} - \frac{24 + z + w}{3(1 + z + w)} \right). \quad (56)$$

The upper bound on the axion-photon coupling is derived from the recent analysis of the horizontal-branch stars in galactic globular clusters [56], which translates into the lower bound of the decay constant through Eq. (53) as

$$|g_{a\gamma\gamma}| < 6.6 \times 10^{-11} \text{ GeV}^{-1} (95\% \text{ CL}) \Leftrightarrow F_A \gtrsim \begin{cases} 3.23 \times 10^7 \text{ GeV} & (\text{Case I}), \\ 2.64 \times 10^7 \text{ GeV} & (\text{Case II}), \\ 8.84 \times 10^6 \text{ GeV} & (\text{Case III}), \end{cases} \quad (57)$$

where on the right-hand side $E/N = 23/6$ (Case I), $1/2$ (Case II), and $5/2$ (Case III) for $z = 0.48$ are used. Subsequently, the bound in Eq. (57) translates into the upper bound of the axion mass through Eq. (53) as $m_a \lesssim 0.17$, $\lesssim 0.21$, and $\lesssim 0.62$ eV for Case I, II, and III, respectively. It is well known that magnetic fields in or behind galaxy clusters convert photons into axions and alter the spectrum of the x-ray photons arriving at the Earth [57,58]. The nonobservation of the x-ray spectral modulations induced by axion-to-photon conversion with data drawn from the Chandra archive has placed a bound on the axion-photon coupling [59]:

$$|g_{a\gamma\gamma}| \lesssim 1.5 \times 10^{-12} \text{ GeV}^{-1} (95\% \text{ CL}) \Leftrightarrow F_A \gtrsim \begin{cases} 1.42 \times 10^9 \text{ GeV} & (\text{Case I}), \\ 1.16 \times 10^9 \text{ GeV} & (\text{Case II}), \\ 3.89 \times 10^8 \text{ GeV} & (\text{Case III}). \end{cases} \quad (58)$$

The bounds of Eqs. (57) and (58) are much lower than that of Eq. (44) coming from the present experimental upper bound $\text{Br}(K^+ \rightarrow \pi^+ A_i) < 7.3 \times 10^{-11}$ [16] as well as the axion-to-electron coupling $6.7 \times 10^{-29} \lesssim \alpha_{\text{Aee}} \lesssim 5.6 \times 10^{-27}$ at 3σ [14].

Hence, from Eqs. (44) and (53) the QCD axion mass and its corresponding axion-photon couplings for $z = 0.48$ predicted by the model are as follows:

$$m_a = 1.54_{-0.29}^{+0.48} \times 10^{-4} \text{ eV} \Leftrightarrow |g_{a\gamma\gamma}| = \begin{cases} 5.99_{-1.14}^{+1.85} \times 10^{-14} \text{ GeV}^{-1} & (\text{Case I}), \\ 4.89_{-0.93}^{+1.51} \times 10^{-14} \text{ GeV}^{-1} & (\text{Case II}), \\ 1.64_{-0.31}^{+0.51} \times 10^{-14} \text{ GeV}^{-1} & (\text{Case III}). \end{cases} \quad (59)$$

Note here that if $0.38 < z < 0.58$ is considered for the given axion mass range, the ranges of $|g_{a\gamma\gamma}|$ in Eq. (59) can become wider than those for $z = 0.48$. The corresponding Compton wavelength of axion oscillation is $\lambda_a = (2\pi\hbar/m_a)c$, with $c \simeq 2.997 \times 10^8$ m/s and $\hbar \simeq 1.055 \times 10^{-34}$ J s:

$$\lambda_a = 8.04_{-1.90}^{+1.90} \text{ mm}. \quad (60)$$

The QCD axion coupling to the photon $g_{a\gamma\gamma}$ divided by the QCD axion mass m_a is dependent on E/N . Figure 1 shows the E/N dependence of $(g_{a\gamma\gamma}/m_a)^2$ so that the experimental limit is independent of the axion mass m_a [8]: for $0.38 < z < 0.58$, the values of $(g_{a\gamma\gamma}/m_a)^2$ for Cases II

and III are located lower than that of the Axion Dark Matter eXperiment (ADMX) bound [13], while for Case I it is marginally¹² lower than that of the ADMX bound, where $(g_{a\gamma\gamma}/m_a)_{\text{ADMX}}^2 \leq 1.44 \times 10^{-19} \text{ GeV}^{-2} \text{ eV}^{-2}$. The gray band represents the experimentally excluded bound $(g_{a\gamma\gamma}/m_a)_{\text{ADMX}}^2$, while the cyan band stands for $0.38 < z < 0.58$. For the Weinberg value $z = 0.48_{-0.10}^{+0.10}$, the anomaly values $E/N = 23/6$, $1/2$, and $5/2$ predict $(g_{a\gamma\gamma}/m_a)^2 = 1.507_{-0.137}^{+0.126} \times 10^{-19} \text{ GeV}^{-2} \text{ eV}^{-2}$ (Case I), $1.003_{-0.368}^{+0.382} \times 10^{-19} \text{ GeV}^{-2} \text{ eV}^{-2}$ (Case II), and $1.128_{-0.252}^{+0.163} \times 10^{-20} \text{ GeV}^{-2} \text{ eV}^{-2}$ (Case III), respectively.

¹²In fact, this is the case for $0.54 \lesssim z < 0.58$.

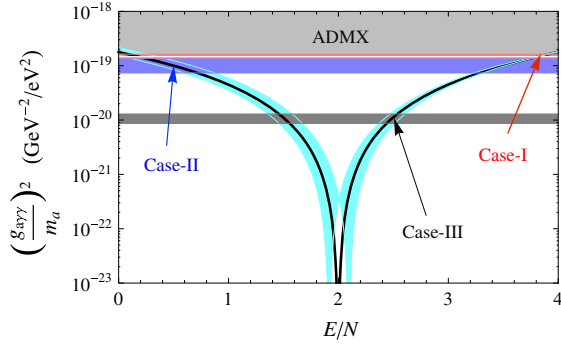


FIG. 1. Plot of $(g_{a\gamma\gamma}/m_a)^2$ versus E/N for $z = 0.48$ (black curve) and $0.38 < z < 0.58$ (cyan band). The gray band represents the experimentally excluded bound $(g_{a\gamma\gamma}/m_a)^2 \leq 1.44 \times 10^{-19} \text{ GeV}^{-2} \text{ eV}^{-2}$ from ADMX [12,13]. Here the horizontal light-red, light-blue, and light-black bands stand for $(g_{a\gamma\gamma}/m_a)^2 = 1.507^{+0.126}_{-0.137} \times 10^{-19} \text{ GeV}^{-2} \text{ eV}^{-2}$ for $E/N = 23/6$, $1.003^{+0.382}_{-0.368} \times 10^{-19} \text{ GeV}^{-2} \text{ eV}^{-2}$ for $E/N = 1/2$, and $1.128^{+0.163}_{-0.252} \times 10^{-20} \text{ GeV}^{-2} \text{ eV}^{-2}$ for $E/N = 5/2$, respectively.

Clearly, as shown in Fig. 1, the uncertainties of $(g_{a\gamma\gamma}/m_a)^2$ for Cases II and III are larger than that of Case I for $0.38 < z < 0.58$.

Figure 2 shows the axion-photon coupling $|g_{a\gamma\gamma}|$ as a function of the axion mass m_a in terms of anomaly values $E/N = 23/6$, $1/2$, and $5/2$ which correspond to Case I, II, and III, respectively. In particular, in the model, for $F_A = 3.56^{+0.84}_{-0.84} \times 10^{10} \text{ GeV}$ and $z = 0.48$ we obtain the QCD axion mass $m_a = 1.54^{+0.48}_{-0.29} \times 10^{-4} \text{ eV}$ and the axion-photon coupling $|g_{a\gamma\gamma}| = 5.99^{+1.85}_{-1.14} \times 10^{-14} \text{ GeV}^{-1}$ (horizontal light-red band), $4.89^{+1.51}_{-0.93} \times 10^{-14} \text{ GeV}^{-1}$ (horizontal light-blue band), and $1.64^{+0.51}_{-0.31} \times 10^{-14} \text{ GeV}^{-1}$ (horizontal light-black band), which correspond to Case I, II, and III, respectively.

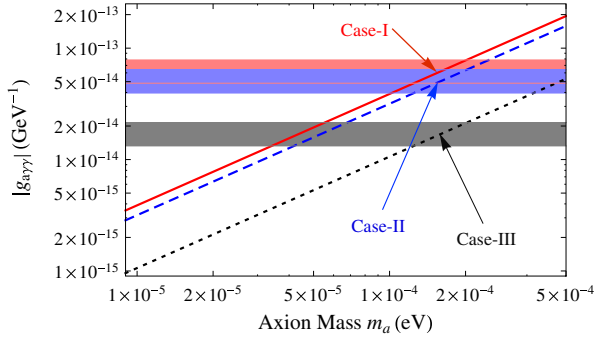


FIG. 2. Plot of $|g_{a\gamma\gamma}|$ versus m_a for Case I (slanted red-solid line), Case II (slanted blue-dashed line), and Case III (slanted black-dotted line) in terms of $E/N = 23/6$, $1/2$, and $5/2$, respectively. In particular, the QCD axion mass $m_a = 1.54^{+0.48}_{-0.29} \times 10^{-4} \text{ eV}$ is equivalent to the axion-photon coupling $|g_{a\gamma\gamma}| = 5.99^{+1.85}_{-1.14} \times 10^{-14} \text{ GeV}^{-1}$ (horizontal light-red band), $4.89^{+1.51}_{-0.93} \times 10^{-14} \text{ GeV}^{-1}$ (horizontal light-blue band), and $1.64^{+0.51}_{-0.31} \times 10^{-14} \text{ GeV}^{-1}$ (horizontal light-black band), which corresponds to Case I, II, and III, respectively.

(horizontal light-blue band), and $1.64^{+0.51}_{-0.31} \times 10^{-14} \text{ GeV}^{-1}$ (horizontal light-black band), which correspond to Case I, II, and III, respectively. As the upper bound on $\text{Br}(K^+ \rightarrow \pi^+ + A_i)$ gets tighter, the range of the QCD axion mass gets narrower, and consequently the corresponding band width for $|g_{a\gamma\gamma}|$ in Fig. 2 gets narrower. In Fig. 2 the top edge of the bands comes from the upper bound on $\text{Br}(K^+ \rightarrow \pi^+ + A_i)$, while the bottom edge of the bands is from the astrophysical constraints of star cooling induced by the flavored-axion bremsstrahlung off electrons, $e + Ze \rightarrow Ze + e + A_i$.

The model will be tested in the very near future through experiments at the Center for Axion and Precision Physics research [60] as well as the NA62 experiment, which is expected to reach a sensitivity of $\text{Br}(K^+ \rightarrow \pi^+ + A_i) < 1.0 \times 10^{-12}$ [46].

IV. SUMMARY AND CONCLUSION

Motivated by the flavored-PQ symmetry to unify flavor physics and string theory [1,7], we have constructed a compact model based on $SL_2(F_3) \times U(1)_X$ symmetry for resolving rather recent, but fast-growing issues in astroparticle physics, including quark and leptonic mixings and CP violations, high-energy neutrinos, the QCD axion, and axion cooling of stars. Since astroparticle physics observations have increasingly placed tight constraints on parameters for flavored axions, we have shown how the scale responsible for the PQ mechanism (congruent to that of the seesaw mechanism) could be fixed, and in turn the scale responsible for the FN mechanism through flavor physics. Along the lines of finding the fundamental scales, the flavored-PQ symmetry together with the non-Abelian finite symmetry is well flavor-structured in a unique way that the domain-wall number $N_{\text{DW}} = 1$ with the $U(1)_X \times [\text{gravity}]^2$ anomaly-free condition demands additional Majorana fermion and the flavor puzzles of SM are well delineated by the new expansion parameters expressed in terms of $U(1)_X$ charges and $U(1)_X - [SU(3)_C]^2$ anomaly coefficients, providing interesting physical implications for neutrinos, the QCD axion, and flavored axions.

In particular, the QCD axion decay constant congruent to the seesaw scale, through its connection to the astroparticle constraints of stellar evolution induced by the flavored-axion bremsstrahlung off electrons $e + Ze \rightarrow Ze + e + A_i$ and the rare flavor-changing decay process induced by the flavored axion $K^+ \rightarrow \pi^+ + A_i$, was shown to be fixed at $F_A = 3.56^{+0.84}_{-0.84} \times 10^{10} \text{ GeV}$. Consequently, the QCD axion mass $m_a = 1.54^{+0.48}_{-0.29} \times 10^{-4} \text{ eV}$, the wavelength of its oscillation $\lambda_a = 8.04^{+1.90}_{-1.90} \text{ mm}$, the axion-to-neutron coupling $g_{\text{Ann}} = 2.14^{+0.66}_{-0.41} \times 10^{-12}$, and the

axion-to-photon coupling $|g_{a\gamma\gamma}| = 5.99^{+1.85}_{-1.14} \times 10^{-14} \text{ GeV}^{-1}$ for $E/N = 23/6$ (Case I), $4.89^{+1.51}_{-0.93} \times 10^{-14} \text{ GeV}^{-1}$ for $E/N = 1/2$ (Case II), and $1.64^{+0.51}_{-0.31} \times 10^{-14} \text{ GeV}^{-1}$ for $E/N = 5/2$ (Case III), respectively, in the case where $z = 4.8$. Subsequently, the scale associated with the FN mechanism is automatically fixed through its connection to the SM fermion masses and mixings, $\Lambda = 2.04^{+0.48}_{-0.48} \times 10^{11} \text{ GeV}$, and such a fundamental scale might give a hint of where some string moduli are stabilized in type IIB string vacua.

In the very near future, the NA62 experiment [which is expected to reach a sensitivity of $\text{Br}(K^+ \rightarrow \pi^+ + A_i) < 1.0 \times 10^{-12}$] will probe the flavored axions or exclude the model.

ACKNOWLEDGMENTS

I would like to give thanks to B. H. An and M. H. Ahn for useful conversations. This work is supported by the National Key Program for Research and Development of China (No. 2016YFA0400200).

-
- [1] Y. H. Ahn, *Phys. Rev. D* **96**, 015022 (2017).
 [2] Y. H. Ahn, arXiv:1706.09707.
 [3] P. Minkowski, *Phys. Lett. B* **67**, 421 (1977).
 [4] R. D. Peccei and H. R. Quinn, *Phys. Rev. Lett.* **38**, 1440 (1977).
 [5] Y. H. Ahn and E. J. Chun, *Phys. Lett. B* **752**, 333 (2016).
 [6] S. L. Cheng, C. Q. Geng, and W. T. Ni, *Phys. Rev. D* **52**, 3132 (1995).
 [7] Y. H. Ahn, *Phys. Rev. D* **93**, 085026 (2016).
 [8] Y. H. Ahn, *Phys. Rev. D* **91**, 056005 (2015).
 [9] C. D. Froggatt and H. B. Nielsen, *Nucl. Phys.* **B147**, 277 (1979).
 [10] I. Esteban, M. C. Gonzalez-Garcia, M. Maltoni, I. Martinez-Soler, and T. Schwetz, *J. High Energy Phys.* **01** (2017) 087.
 [11] M. G. Aartsen *et al.* (IceCube Collaboration), *Science* **342**, 1242856 (2013); *Phys. Rev. Lett.* **113**, 101101 (2014); **114**, 171102 (2015).
 [12] S. J. Asztalos *et al.* (ADMX Collaboration), *Phys. Rev. Lett.* **104**, 041301 (2010).
 [13] S. J. Asztalos *et al.*, *Phys. Rev. D* **69**, 011101 (2004).
 [14] M. Giannotti, I. G. Irastorza, J. Redondo, A. Ringwald, and K. Saikawa, *J. Cosmol. Astropart. Phys.* **10** (2017) 010.
 [15] A. Ringwald, *Proc. Sci.*, NEUTEL2015 (2015) 021 [arXiv:1506.04259]; M. Giannotti, arXiv:1508.07576; M. Giannotti, I. Irastorza, J. Redondo, and A. Ringwald, *J. Cosmol. Astropart. Phys.* **05** (2016) 057.
 [16] S. Adler *et al.* (E949 and E787 Collaborations), *Phys. Rev. D* **77**, 052003 (2008).
 [17] Y. H. Ahn, arXiv:1802.05044.
 [18] M. B. Green and J. H. Schwarz, *Phys. Lett. B* **149**, 117 (1984).
 [19] Y. Ema, D. Hagihara, K. Hamaguchi, T. Moroi, and K. Nakayama, *J. High Energy Phys.* **04** (2018) 094; F. Bjrkereth, E. J. Chun, and S. F. King, *Phys. Lett. B* **777**, 428 (2018); F. Arias-Aragon and L. Merlo, *J. High Energy Phys.* **10** (2017) 168; J. C. Gmez-Izquierdo, *Eur. Phys. J. C* **77**, 551 (2017); Y. Ema, K. Hamaguchi, T. Moroi, and K. Nakayama, *J. High Energy Phys.* **01** (2017) 096; L. Calibbi, F. Goertz, D. Redigolo, R. Ziegler, and J. Zupan, *Phys. Rev. D* **95**, 095009 (2017); T. Nomura, Y. Shimizu, and T. Yamada, *J. High Energy Phys.* **06** (2016) 125.
 [20] F. Feruglio, C. Hagedorn, Y. Lin, and L. Merlo, *Nucl. Phys.* **B775**, 120 (2007).
 [21] K. M. Case, R. Karplus, and C. N. Yang, *Phys. Rev.* **101**, 874 (1956); P. H. Frampton and T. W. Kephart, *Int. J. Mod. Phys. A* **10**, 4689 (1995).
 [22] A. Aranda, C. D. Carone, and R. F. Lebed, *Phys. Lett. B* **474**, 170 (2000); A. Aranda, C. D. Carone, and R. F. Lebed, *Phys. Rev. D* **62**, 016009 (2000); C. D. Carone, S. Chaurasia, and S. Vazquez, *Phys. Rev. D* **95**, 015025 (2017).
 [23] L. M. Krauss and F. Wilczek, *Phys. Rev. Lett.* **62**, 1221 (1989).
 [24] Y. H. Ahn and P. Gondolo, *Phys. Rev. D* **91**, 013007 (2015).
 [25] G. Altarelli and F. Feruglio, *Nucl. Phys.* **B720**, 64 (2005); **B741**, 215 (2006); *Rev. Mod. Phys.* **82**, 2701 (2010).
 [26] L. Wolfenstein, *Phys. Rev. D* **18**, 958 (1978); P. F. Harrison, D. H. Perkins, and W. G. Scott, *Phys. Lett. B* **530**, 167 (2002); P. F. Harrison and W. G. Scott, *Phys. Lett. B* **535**, 163 (2002); **557**, 76 (2003).
 [27] J. Gehrlein and M. Spinrath, *Eur. Phys. J. C* **77**, 281 (2017); J. Gehrlein, A. Merle, and M. Spinrath, *Phys. Rev. D* **94**, 093003 (2016).
 [28] Y. H. Ahn, S. K. Kang, and C. S. Kim, *J. High Energy Phys.* **10** (2016) 092.
 [29] L. Wolfenstein, *Phys. Rev. Lett.* **51**, 1945 (1983).
 [30] Y. H. Ahn, H. Y. Cheng, and S. Oh, *Phys. Lett. B* **703**, 571 (2011).
 [31] <http://ckmfitter.in2p3.fr>.
 [32] C. Patrignani *et al.* (Particle Data Group), *Chin. Phys. C* **40**, 100001 (2016) and 2017 update.
 [33] L. L. Chau and W. Y. Keung, *Phys. Rev. Lett.* **53**, 1802 (1984).
 [34] S. Antusch, J. Kersten, M. Lindner, M. Ratz, and M. A. Schmidt, *J. High Energy Phys.* **03** (2005) 024.
 [35] E. Aprile *et al.* (XENON100 Collaboration), *Phys. Rev. D* **90**, 062009 (2014); **95**, 029904(E) (2017).
 [36] C. Fu *et al.* (PandaX Collaboration), *Phys. Rev. Lett.* **119**, 181806 (2017).
 [37] J. Redondo, *J. Cosmol. Astropart. Phys.* **12** (2013) 008.
 [38] N. Viaux, M. Catelan, P. B. Stetson, G. G. Raffelt, J. Redondo, A. A. R. Valcarce, and A. Weiss, *Phys. Rev. Lett.* **111**, 231301 (2013).
 [39] G. G. Raffelt, *Phys. Lett. B* **166**, 402 (1986); S. I. Blinnikov and N. V. Dunina-Barkovskaya, *Mon. Not. R. Astron. Soc.* **266**, 289 (1994).

- [40] M. M. Miller Bertolami, B. E. Melendez, L. G. Althaus, and J. Isern, *J. Cosmol. Astropart. Phys.* **10** (2014) 069.
- [41] H. Umeda, N. Iwamoto, S. Tsuruta, L. Qin, and K. Nomoto, [arXiv:astro-ph/9806337](https://arxiv.org/abs/astro-ph/9806337); J. Keller and A. Sedrakian, *Nucl. Phys.* **A897**, 62 (2013).
- [42] G. G. Raffelt, *Astrophys. J.* **365**, 559 (1990); G. Raffelt and A. Weiss, *Phys. Rev. D* **51**, 1495 (1995); G. G. Raffelt, *Lect. Notes Phys.* **741**, 51 (2008); G. G. Raffelt, J. Redondo, and N. V. Maira, *Phys. Rev. D* **84**, 103008 (2011).
- [43] F. Wilczek, *Phys. Rev. Lett.* **49**, 1549 (1982).
- [44] R. D. Bolton *et al.*, *Phys. Rev. D* **38**, 2077 (1988).
- [45] G. G. Raffelt, *Stars as Laboratories for Fundamental Physics: The Astrophysics of Neutrinos, Axions, and Other Weakly Interacting Particles* (University of Chicago, Chicago, 1996).
- [46] R. Fantechi (NA62 Collaboration), [arXiv:1407.8213](https://arxiv.org/abs/1407.8213).
- [47] J. Isern, E. Garcia-Berro, S. Torres, and S. Catalan, *Astrophys. J.* **682**, L109 (2008); J. Isern, S. Catalan, E. Garcia-Berro, and S. Torres, *J. Phys. Conf. Ser.* **172**, 012005 (2009); J. Isern, M. Hernanz, and E. Garcia-Berro, *Astrophys. J.* **392**, L23 (1992).
- [48] J. Isern, E. Garcia-Berro, L. G. Althaus, and A. H. Corsico, *Astron. Astrophys.* **512**, A86 (2010); A. H. Corsico, L. G. Althaus, M. M. M. Bertolami, A. D. Romero, E. Garcia-Berro, J. Isern, and S. O. Kepler, *Mon. Not. R. Astron. Soc.* **424**, 2792 (2012); A. H. Corsico, L. G. Althaus, A. D. Romero, A. S. Mukadam, E. Garcia-Berro, J. Isern, S. O. Kepler, and M. A. Corti, *J. Cosmol. Astropart. Phys.* **12** (2012) 010; J. Isern, E. Garcia-Berro, S. Torres, and S. Catalan, *Astrophys. J.* **682**, L109 (2008); J. Isern, S. Catalan, E. Garcia-Berro, and S. Torres, *J. Phys. Conf. Ser.* **172**, 012005 (2009); J. Isern *et al.*, [arXiv:1204.3565](https://arxiv.org/abs/1204.3565); B. Melendez, M. M. Bertolami, and L. Althaus, *ASP Conf. Ser.* **469**, 189 (2013).
- [49] J. L. Feng, T. Moroi, H. Murayama, and E. Schnapka, *Phys. Rev. D* **57**, 5875 (1998).
- [50] A. V. Artamonov *et al.* (E949 Collaboration), *Phys. Rev. Lett.* **101**, 191802 (2008); A. V. Artamonov *et al.* (BNL-E949 Collaboration), *Phys. Rev. D* **79**, 092004 (2009).
- [51] G. Grilli di Cortona, E. Hardy, J. Pardo Vega, and G. Villadoro, *J. High Energy Phys.* **01** (2016) 034.
- [52] A. Sedrakian, *Phys. Rev. D* **93**, 065044 (2016).
- [53] L. B. Leinson, *J. Cosmol. Astropart. Phys.* **08** (2014) 031.
- [54] L. B. Leinson, *Phys. Lett. B* **741**, 87 (2015).
- [55] H. Leutwyler, *Phys. Lett. B* **378**, 313 (1996).
- [56] A. Ayala, I. Domnguez, M. Giannotti, A. Mirizzi, and O. Straniero, *Phys. Rev. Lett.* **113**, 191302 (2014).
- [57] P. Sikivie, *Phys. Rev. Lett.* **51**, 1415 (1983); **52**, 695(E) (1984).
- [58] G. Raffelt and L. Stodolsky, *Phys. Rev. D* **37**, 1237 (1988).
- [59] J. P. Conlon, F. Day, N. Jennings, S. Krippendorf, and M. Rummel, *J. Cosmol. Astropart. Phys.* **07** (2017) 005.
- [60] Center for Axion and Precision Physics Research, http://capp.ibs.re.kr/html/capp_en/.